Journal of Anatomy

J. Anat. (2014) **225**, pp419–435 doi: 10.1111/joa.12221

Anatomical landmarks for the localization of the greater palatine foramen – a study of 1200 head CTs, 150 dry skulls, systematic review of literature and meta-analysis

Iwona M. Tomaszewska,[1] Krzysztof A. Tomaszewski,[2] Elizabeth K. Kmiotek,[2] Iwona Z. Pena,[2] Andrzej Urbanik,[3] Michał Nowakowski[1] and Jerzy A. Walocha[2]

[1]*Department of Medical Education, Jagiellonian University Medical College, Krakow, Poland*
[2]*Department of Anatomy, Jagiellonian University Medical College, Krakow, Poland*
[3]*Department of Radiology, Jagiellonian University Medical College, Krakow, Poland*

Abstract

Accurate knowledge of greater palatine foramen (GPF) anatomy is necessary when performing a variety of anaesthesiological, dental or surgical procedures. The first aim of this study was to localize the GPF in relation to multiple anatomical landmarks. The second aim was to perform a systematic review of literature, and to conduct a meta-analysis on the subject of GPF position to aid clinicians in their practice. One-hundred and fifty dry, adult, human skulls and 1200 archived head computed tomography scans were assessed and measured in terms of GPF relation to other anatomical reference points. A systematic literature search was performed using the PubMed, Embase and Web of Science databases, and a meta-analysis on the subject of GPF relation to the maxillary molars was conducted. On average, in the Polish population, the GPF was positioned 15.9 ± 1.5 mm from the midline maxillary suture (MMS), 3.0 ± 1.2 mm from the alveolar ridge (AR) and 17.0 ± 1.5 mm from the posterior nasal spine (PNS); 74.7% of GPF were positioned opposite the third maxillary molar (M3). Twenty-seven studies were included in the systematic review and 23 in the meta-analysis ($n = 6927$ GPF). The pooled prevalence of the GPF being positioned opposite the M3 was 63.9% (95% confidence interval = 56.6–70.9%). Concluding, the GPF is most often located opposite the M3 in the majority of the world's populations. The maxillary molars are the best landmarks for locating the GPF. In edentulous patients the most useful points for approximating the position of the GPF are the AR, MMS and PNS. This study introduces an easy and repeatable classification to reference the GPF to the maxillary molars.

Key words: anatomy; greater palatine foramen; meta-analysis; position; systematic review.

Introduction

The maxillary nerve and its tributaries provide sensory innervation to the maxillary teeth, the palate, the nasal cavity, the sinuses and subsequently the skin of the midface (Howard-Swirzinski et al. 2010). The maxillary nerve originates from the trigeminal ganglion, passes through the cavernous sinus, proceeds to exit through the foramen rotundum, and finally enters the pterygopalatine fossa where it gives rise to multiple branches (Rodella et al. 2012). The anterior (greater) palatine nerve supplies the main sensory innervation to the palate. It branches off the maxillary nerve and passes through the greater palatine canal (GPC) to surface on the hard palate from the greater palatine foramen (GPF), and continues anteriorly, ending just short of the front incisors (Sharma & Garud, 2013).

The anterior palatine nerve block was first described in 1927 (Ikuta et al. 2013). This procedure can be performed using two intra-oral approaches – the high tuberosity approach or the GPC approach (Piagkou et al. 2012). The latter is associated with a higher success rate and a lower incidence of complications (Wong & Sved, 1991). However, the major clinical difficulty of this method is to accurately locate the position of the GPF, which is the palatal exit point of the GPC (Wong & Sved, 1991). The GPC approach is of additional clinical significance as it allows to reduce bleeding during nasal septum surgical repair (Mercuri, 1979), endoscopic sinus surgery and septorhinoplasty

Correspondence
Iwona M. Tomaszewska, DDS, Department of Medical Education, Jagiellonian University Medical College, 16 Lazarza Street, 31-530 Kraków, Poland. T: +48-666-666-987; E: im.tomaszewska@gmail.com

This work has been partially presented at the I Congress of the Polish Anatomical Society, Dolina Charlotty, 27–30.06.2013, and received the Congress 'Young Investigator' award.

Accepted for publication *30 June 2014*
Article published online *5 August 2014*

(Das et al. 2006; Douglas & Wormald, 2006). What is more, accurate GPF localization is needed when aiming to mobilize the greater palatine artery during oroantral fistulae closure using mucoperiosteal pedicled palatal flaps (Bell, 2011; Piagkou et al. 2012) or during palatal mucosa graft harvesting for periodontal proposes (Klosek & Rungruang, 2009). All of the above underline the essential need to thoroughly understand the anatomy and anatomical variability of the GPF and its associated landmarks.

Matsuda (1927) was the first to report on the localization of the GPF. The majority of textbooks still locate the GPF in a very general way, for example near the lateral or posterolateral palatal border, medial or opposite the third maxillary molar (M3; Romanes, 1981). Anaesthesia textbooks seem to be a little more specific in that matter, loosely positioning the GPF in relation to the maxillary molars (Shane, 1975).

Up-to-date, anatomical studies on the placement of the GPF have been conducted in numerous populations, such as African (Langenegger et al. 1983; Hassanali & Mwaniki, 1984; Ajmani, 1994; Osunwoke et al. 2011), American (Malamed & Trieger, 1983; Fu et al. 2011), Brazilian (Chrcanovic BR & Custódio, 2010; Teixeira et al. 2010; Urbano et al. 2010; Lopes et al. 2011; Ikuta et al. 2013), Chinese (Wang et al. 1988), European (Malamed & Trieger, 1983; Piagkou et al. 2012; Nimigean et al. 2013), Indian (Westmoreland & Blanton, 1982; Ajmani, 1994; Sujatha et al. 2005; Saralaya & Nayak, 2007; Kumar et al. 2011; D'Souza et al. 2012; Dave et al. 2013; Jotania et al. 2013; Sharma & Garud, 2013), Korean (Lee et al. 2001; Hwang et al. 2011) and Thai (Methathrathip et al. 2005; Klosek & Rungruang, 2009). However, the main limitation of all of the previously mentioned studies is that they were conducted on a very limited number of subjects/samples, not exceeding 300 skulls or 50 computed tomography (CT) scans or cone-beam CT scans. Even the most recent studies (Ikuta et al. 2013) see the need for further investigation to establish an exact reference point or position of the GPF. The growing number of publications on the subject of GPF position makes it difficult for a clinician to draw practical conclusions, especially when some of the studies present conflicting results.

Thus, the first aim of the present study was to localize the GPF relative to multiple anatomical landmarks in a large sample of Polish adult skulls and head CTs. The second aim of the study was to perform a comprehensive review of literature on the subject of GPF position, and to conduct a meta-analysis on the prevalence of GPF location in regard to the maxillary molars to aid clinicians in their practice.

Materials and methods

Study materials

The present study was conducted on 150 dry, adult, sexed, human skulls obtained from the Museum of the Department of Anatomy cranial collection (Jagiellonian University Medical College – http://www.katedra-anatomii.cm-uj.krakow.pl/?q=muzeum-katedry) and 1200 archived adult head CT scans (Department of Radiology, Jagiellonian University Medical College and Department of Radiology and J. Dietl's Specialistic Hospital, Krakow, Poland). Data regarding sex and age of the analysed dry skulls were obtained from the records of the Museum of the Department of Anatomy.

The CT images were acquired using a Siemens Somatom Sensation 16 and a Toshiba Aquilion 64. The following study parameters were applied: exposure 120 kV, 74 mA, 60 mAs; rotation time: 0.5 s; slice thickness: 0.5 mm. Patient's sex and age data were acquired from patient files.

Study inclusion criteria were full eruption of third molars on both sides of the maxilla, presence of all maxillary teeth, participant/specimen age over 21 years, and absence of any pathological (including developmental and traumatic) changes in the region of the maxilla.

Measurements

The measurements were performed using a digital caliper (Mitutoyo, Japan; dry skulls) or the eFilm Workstation 3.4 (Merge Healthcare; CT scans). For the CT scans, maximum intensity projections, multi-planar reconstructions and volume rendering reconstructions were examined in three planes: coronal; sagittal; and transverse. All measurements were recorded to the nearest 0.01 mm, and after statistical analysis were rounded up to the nearest 0.1 mm for data presentation. All bilateral measurements were performed symmetrically. Each measurement was taken twice by the same observer and, in cases of any discrepancies, the mean of the two values was recorded. After all of the samples were measured, 20% of randomly chosen samples were re-measured by an observer who did not partake in assessing the samples the first time. Interclass correlations (ICCs) were calculated. The level of agreement between the assessments was very high (ICC = 0.92–0.96).

The centre of the GPF was established while measuring its anterior–posterior (AP) and lateral–medial (LM) dimensions. GPF centre was set at the point of the intersection of two straight lines representing the longest AP and LM GPF dimensions. If necessary this was corrected visually, using the GPF form factor. The form factor was obtained by dividing the AP by LM dimensions. If the GPF was circular in shape, the obtained value was equal to 1. Values > 1 indicated an AP elongated GPF, and values < 1 indicated a LM elongated foramen (Jaffar & Hamadah, 2003).

The following assessments were performed (Fig. 1).

1 Measurements from the centre of the GPF: shortest perpendicular distance to the midline maxillary suture (MMS); shortest distance to the posterior border of the hard palate (PBHP), to the centre of the incisive foramen (IF), to the alveolar ridge (AR), to the tip of the pterygoid hamulus (PH), to the posterior nasal spine (PNS), to the centres of the second maxillary molar (M2) and the M3, and to the centre of the opposite GPF.
2 Measurement of the MMS–IF–GPF angle, maximal palatal vault height (at the level of the second molar a perpendicular line was drawn from the AR level to the MMS), palatal vault breadth (at the level of the second molars) and palatal vault length (distance between the orale and staphylion points).
3 Evaluation of the presence of the GPF posterior palatine crest and the number of lesser palatine foramen (LPFs), as well as palatal vault shape.
4 Evaluation of GPF opening direction, and GPF position in relation to the maxillary molars (a perpendicular line from the

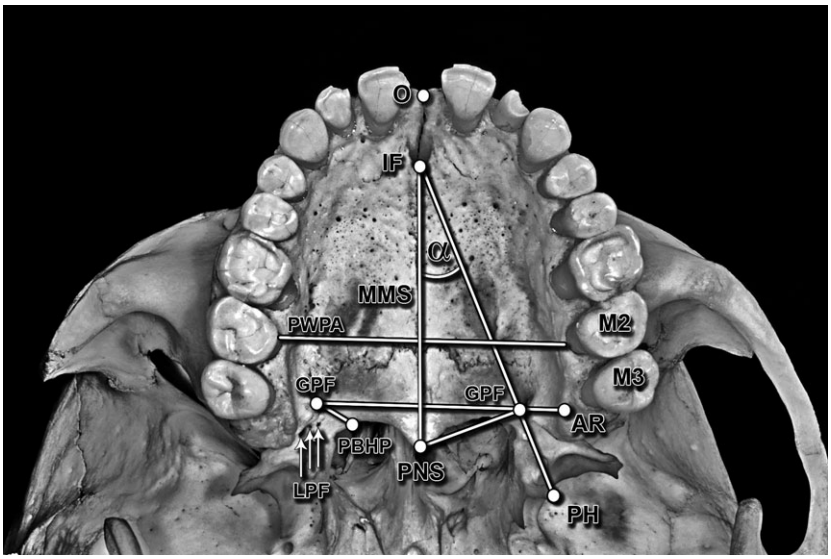

Fig. 1 Ventral photograph of the hard palate illustrating performed measurements. O, orale; IF, incisive foramen; MMS, midline maxillary suture; PWPA, posterior width of the palatal arch; GPF, greater palatine foramen; LPF, lesser palatine foramina; PBHP, posterior border of the hard palate; PNS, posterior nasal spine; AR, alveolar ridge; PH, tip of the pterygoid hamulus; M2, second maxillary molar; M3, third maxillary molar; α, the PNS–IF–GPF angle.

GPF to the MMS was drawn, and later extended to the maxillary molars).

5 Calculation of the palatine index (palatine breadth to palatine length ratio expressed as a percentage) and the palatal height index (palatine height to palatine breadth ratio expressed as a percentage).

Literature search

This study strictly adhered to the Preferred Reporting Items for Systematic Reviews and Meta-analysis (PRISMA) and Meta-analysis of Observational Studies in Epidemiology (MOOSE) guidelines. The whole process is depicted in Fig. 2. Embase, PubMed and Web of Science databases were searched, by two independent reviewers, for appropriate studies published up to 27 February 2014, without a lower date limit. Search keywords included 'greater', 'palatine' and 'foramen' in different combinations. Review of full-text articles was limited to the ones published in English. References of the identified articles were searched manually. Study inclusion criteria were: studies conducted on human skulls/head CT scans; participants age $\geq$21 years; full-text original articles only (excluding conference abstracts and review papers); $\geq$3 relevant GPF measurements. Inclusion or exclusion of studies was performed hierarchically based on the title of the report first, followed by the abstract, and finally by the full text.

One study was not included in this review as neither the author nor the Journal supplied an abstract or a full copy of the manuscript (Aterkar et al. 1995).

Data extraction and quality assessment were performed independently by two reviewers. The following data were extracted from the relevant studies: citation details; sample size and sample characteristics; as well as relevant measurements performed. In the present meta-analysis the relation of the GPF to the maxillary molars was analysed.

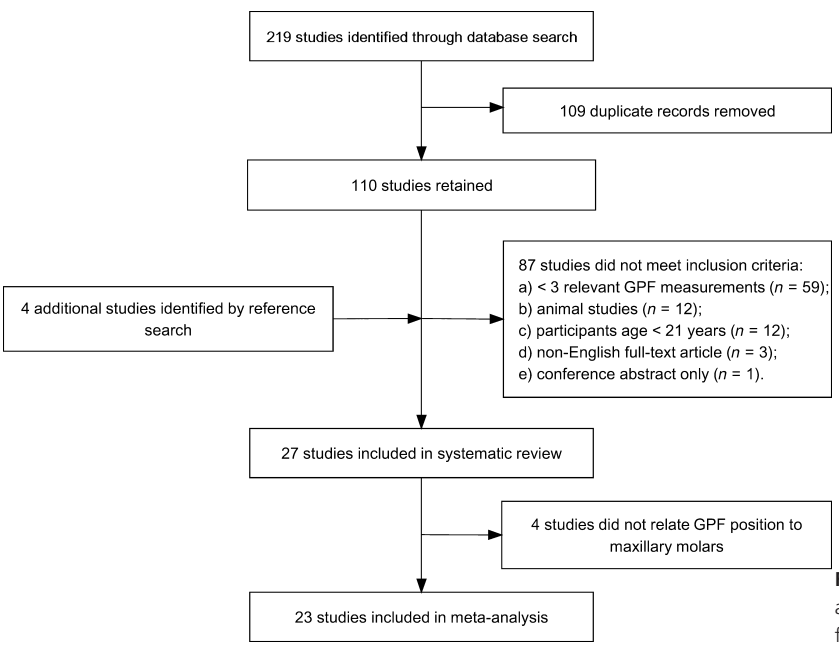

Fig. 2 Flow-chart depicting literature search and study selection. GPF, greater palatine foramen.

Table 1 Main measurements performed on the studied group.

	Females ($n = 695$) Mean (SD) (mm)			Males ($n = 655$) Mean (SD) (mm)				Total ($n = 1350$) Mean (SD) (mm)			
	R	L	T	R	L	T	*P*-value*	R	L	T	*P*-value†
Age (years)	45.4 (16.6)‡			44.4 (17.7)‡			0.28	44.9 (17.1)‡			–
GPF–MMS	15.7 (1.5)	15.4 (1.4)	15.5 (1.5)	16.4 (1.5)	16.0 (1.5)	16.2 (1.5)	$P < 0.0001$	16.1 (1.5)	15.6 (1.5)	15.9 (1.5)	$P < 0.0001$
GPF–PBHP	4.8 (1.0)	4.7 (1.1)	4.7 (1.0)	4.9 (1.0)	4.9 (1.0)	4.9 (1.0)	$P = 0.0002$	4.9 (1.0)	4.8 (1.0)	4.8 (1.0)	$P = 0.25$
GPF–IF	33.2 (2.5)	33.4 (2.7)	33.3 (2.6)	34.8 (3.3)	35.3 (3.3)	35.0 (3.3)	$P < 0.0001$	34.0 (3.0)	34.3 (3.1)	34.2 (3.0)	$P = 0.004$
MMS–IF–GPF angle (°)	26.8 (2.9)	26.3 (2.9)	26.5 (2.9)	25.5 (2.8)	25.7 (3.0)	25.6 (2.9)	$P < 0.0001$	26.0 (2.9)	26.3 (3.0)	26.2 (2.9)	$P = 0.002$
GPF–AR	2.9 (1.4)	2.9 (1.5)	2.9 (1.4)	3.1 (1.2)	2.9 (1.1)	3.0 (1.1)	$P = 0.11$	3.0 (1.3)	2.9 (1.3)	3.0 (1.2)	$P = 0.22$
GPF–PH tip	11.6 (0.8)	11.6 (0.8)	11.6 (0.8)	12.2 (1.2)	12.3 (1.4)	12.2 (1.3)	$P < 0.0001$	11.9 (1.0)	12.0 (1.1)	11.9 (1.1)	$P = 0.19$
GPF–PNS	16.5 (1.2)	16.5 (1.3)	16.5 (1.2)	17.4 (1.5)	17.5 (1.5)	17.4 (1.5)	$P < 0.0001$	17.0 (1.4)	17.0 (1.5)	17.0 (1.5)	$P = 0.48$
GPF–M2	11.3 (2.2)	11.4 (1.9)	11.4 (2.0)	12.2 (2.4)	12.2 (2.3)	12.2 (2.3)	$P < 0.0001$	11.8 (2.1)	11.8 (2.1)	11.8 (2.1)	$P = 0.72$
GPF–M3	11.0 (2.1)	11.0 (1.7)	11.0 (1.9)	11.4 (2.1)	11.7 (2.4)	11.5 (2.2)	$P < 0.0001$	11.3 (2.1)	11.4 (2.1)	11.3 (2.1)	$P = 0.16$
GPF–GPF	28.7 (2.5)‡			29.5 (2.6)‡			$P < 0.0001$	29.1 (2.6)‡			–
Palatal vault height	12.1 (2.5)‡			14.2 (2.5)‡			$P < 0.0001$	13.1 (2.7)‡			–
Palatal vault breadth	45.7 (3.0)‡			48.1 (3.1)‡			$P < 0.0001$	46.9 (3.3)‡			–
Palatal vault length	45.0 (3.9)‡			49.1 (4.2)‡			$P < 0.0001$	47.0 (4.5)‡			–
PI	101.6 (4.7)			98.0 (6.0)			$P < 0.0001$	99.8 (5.4)‡			–
PHI	26.5 (2.9)			29.5 (3.7)			$P < 0.0001$	30.1 (3.1)‡			–

AR, alveolar ridge; GPF, greater palatine foramen; IF, incisive foramen; L, left side; M2, second maxillary molar; M3, third maxillary molar; MMS, midline maxillary suture; PBHP, posterior border of the hard palate; PH, pterygoid hamulus; PHI, palatine height index; PI, palatine index; PNS, posterior nasal spine; R, right side; SD, standard deviation; T, value for both sides.
Palatine index: palatine breadth to palatine length ratio (%); palatine height index: palatine height to palatine breadth ratio (%).
Palatine breadth: measured at the level of maxillary second molars. Palatine length: distance between the orale and staphylion points.
**P*-value for the comparison between female and male total values.
†*P*-value for the comparison between total right and left values.
‡Total value only.

Statistical analysis

Statistical analysis was conducted using Statistica 10 PL (Statistica, Poland) and the MIX 2.0 PRO (BiostatXL) meta-analysis plugin for Excel. Elements of descriptive statistics were used (mean, standard deviation, percentage distribution). Side-related differences were evaluated using the Mann–Whitney *U*-test or the Student's *t*-test as appropriate. ICC was used to evaluate the level of agreement between measurement and re-measurement of the same sample.

Study heterogeneity was assessed using the Cochran *Q*-test and the I^2 index. Values of about 25%, 50% and 75% were interpreted as low, medium and high heterogeneity, respectively. If substantial heterogeneity was observed the random-effects model was used (Huedo-Medina et al. 2006). In case significant heterogeneity was observed, a study subgroup analysis was planned (studies grouped by geographical region). Funnel plot was used to graphically evaluate publication bias (Egger et al. 1997), while statistical assessment of publication bias was conducted through the Egger's and Begg's tests. For each study included in the meta-analysis, the 95% confidence interval for prevalence of the GPF being located opposite the M3 was calculated using the binomial distribution.

A *P*-value of < 0.05 was considered statistically significant.

Ethics

This study has been approved by the Jagiellonian University Medical College Bioethics Committee (registry no. KBET/161/B/

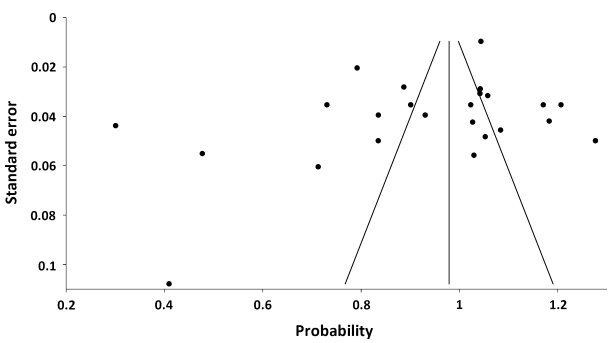

Fig. 3 Funnel plot presenting study heterogeneity and potential publication bias. Each dot depicts an included study. Both Egger's test ($P = 0.16$) and Begg's test ($P = 0.21$) do not indicate the presence of study bias.

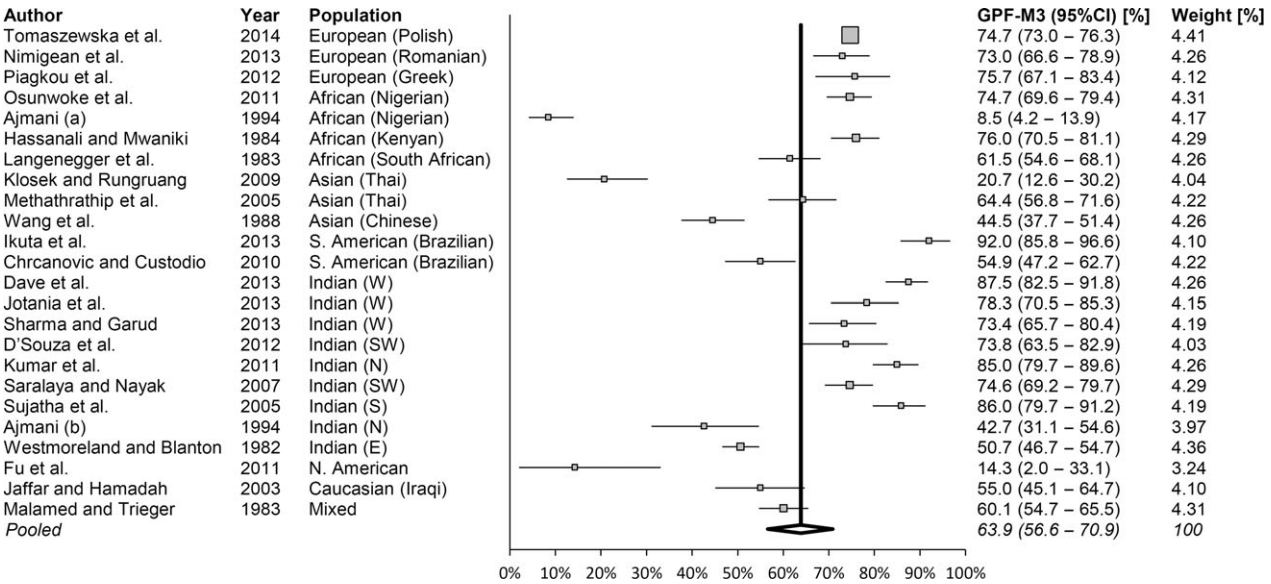

Fig. 4 Forest plot showing studies ($n = 23$) that report on the prevalence of the greater palatine foramen (GPF) being positioned opposite to the third maxillary molar (M3; $Q = 744.7$; $P < 0.0001$ and $I^2 = 96.91\%$). Note: weights were calculated using random-effects analysis. Total number of GPF in the analysis $n = 6927$. GPF–M3, the GPF being opposite to the M3. N, north; S, south; E, east; W, west; CI, confidence interval.

2013), and has been performed in accordance with the ethical standards laid down in the 1964 Declaration of Helsinki and its later amendments.

Results

The studied group comprised 150 dry human skulls and 1200 head CTs – yielding a total of 1350 samples (695 female; 51.5%). The mean age of the group was 44.9 ± 17.1 years – females (45.4 ± 16.6 years) vs. males (44.4 ± 17.7 years; $P = 0.28$). As the measurements performed on dry skulls closely corresponded with those made on the CT scans (ICC = 0.93–97), it was decided that both groups will be treated as one during statistical analysis.

The main measurements performed are presented in Table 1. Overall, the table shows that palate measurements differ significantly between sexes. On the other hand, the right and left sides seem to be symmetrical, taking into account most of the measurements. Table 2 presents the GPF position in relation to the maxillary molars across different studies. Tables 3 and 4 present additional data regarding the position of the GPF and the anatomy of the hard palate obtained from the present study, and at the same time contrast those data with the results of other studies.

Figure 2 presents a flowchart depicting the results of the literature search. Out of the 27 studies included in the systematic review (Tables 2–4), only 23 ($n = 6927$ GPF) were

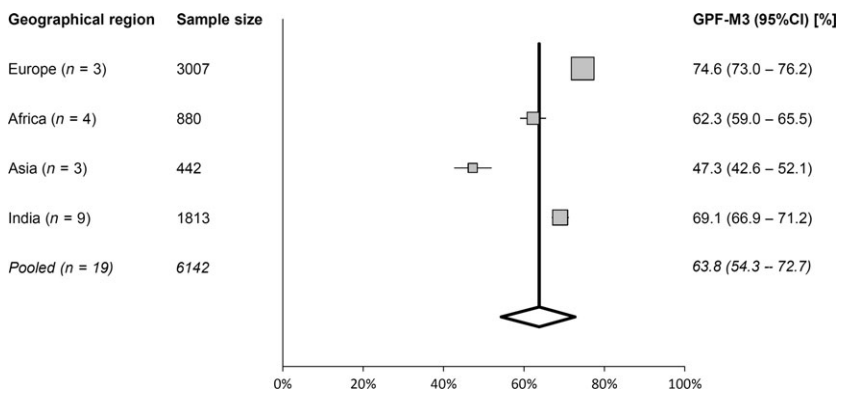

Fig. 5 Forest plot showing studies pooled into the geographical region they originated from, and reporting on the prevalence of the greater palatine foramen (GPF) being positioned opposite to the third molar (M3; $Q = 151.5$; $P < 0.0001$ and $I^2 = 98.02\%$). Note: weights were calculated using random-effects analysis. Sample size: number of GPF in the sample. Studies not included in this analysis are Malamed & Trieger (1983), Jaffar & Hamadah (2003), Chrcanovic & Custudio (2010), Fu et al. (2011) and Ikuta et al. (2013). CI, confidence interval.

Table 2 Data comparison between studies regarding GPF position in relation to the maxillary molars.

Study	Population (number of GPF in the sample)	GPF position (%)																	
		Anterior to M2			Opposite M2			Between M2 and M3			Medial to M3			Opposite M3			Distal to M3		
		R	L	Total	R	L	Total	R	L	Total	R	L	Total	R	L	Total	R	L	Total
European studies (total GPF n = 3007)																			
Tomaszewska et al. 2014 (this study)	Polish (n = 2700)	–			15.5	17.1	16.3	6.8	6.8	6.8	–			75.4	74.0	74.7	1.1	1.1	2.2
Nimigean et al. 2013	Romanian (n = 200)			–			9.0*			15.0*			–			73.0*			3.0*
Piagkou et al. 2012	Greek (n = 107)	–			16.6	17.0	16.8	–			–			76.9	75.5	75.7	7.4	7.5	7.5
African studies (total GPF n = 880)																			
Osunwoke et al. 2011	Nigerian (n = 300)	–			1.3	0.7	1.0	23.3	22.0	22.7	–			74.0	75.3	74.7	1.3	2.0	1.7
Ajmani, 1994	Nigerian (n = 130)	–			10.8	15.4	13.1	36.9	40.0	38.5	43.1	36.9	40.0	9.2	7.7	8.5	–		
Hassanali & Mwaniki, 1984	Kenyan (n = 250)			–			10.4*			13.6*			–			76.0*			–
Langenegger et al. 1983	South African (n = 200)			–	–	1.0	0.5	–	1.0	0.5	–	2.0	1.0	61.0	62.0	61.5	39.0	34.0	36.5
Asian studies (total GPF n = 530)																			
Klosek & Rungruang, 2009	Thai (n = 82)			(F): 14.3* (M): 0			(F): 35.7*, † (M): 65.0*, †			(F): 35.7%* (M): 10.0*			–			(F): 14.3* (M): 25.0*			–
Methathrathip et al. 2005	Thai (n = 160)			0.0*			5.6*, †			23.1*			–			64.4*, †			6.9*
Wang et al. 1988	Chinese (Taiwan) (n = 200)	0.0‡	2.0‡	1.0	14.0	20.0	17	46.0	51.0	48.5	–			40.0	27.0	44.5	–		
Brazilian studies (total GPF n = 260)																			
Ikuta et al. 2013	Brazilian (n = 100)			–			–			–			3.0*			92*			5*
Chrcanovic and Custodio, 2010	Brazilian (n = 160)			–			–			6.2*			–			54.9*			38.9*
Indian studies (total GPF n = 1813)																			
Dave et al. 2013	Indian (W) (n = 200)	–			–			6.0	1.0	3.5	–			88.0¶	94.0¶	87.5¶	12.0	4.0	8.0
Jotania et al. 2013	Indian (W) (n = 120)	–			5.0	3.3	4.2	23.3	11.7	17.5	–			71.7	85.0	78.3	–		
Sharma & Garud, 2013	Indian (W) (n = 139)	–			8.7§	8.7§	8.6	–			–			69.6§	77.1§	73.4	21.7	14.3	18.0
D'Souza et al. 2012	Indian (SW) (n = 80)	–			2.5	2.5	2.5	22.5	25	23.8	–			75.0	72.5	73.8	–		
Kumar et al. 2011	Indian (N) (n = 200)	–			5.0	5.0	5.0	9.0	9.0	9.0	–			85.0	85.0	85.0	1.0	1.0	1.0
Saralaya & Nayak, 2007	Indian (SW) (n = 264)	–			0.8	0	0.4	25	23.5	24.2	–			73.5	75.8	74.6	0.8	0.8	0.8
Sujatha et al. 2005	Indian (S) (n = 142)			–			0.9*			13.1*			–			86.0			–
Ajmani, 1994	Indian (N) (n = 68)	–			–			29.4	35.3	32.4	26.5	17.6	22.1	41.2	44.1	42.7	2.9	2.9	2.9
Westmoreland & Blanton, 1982	Indian (E) (n = 600)	–			8.7	10.6	9.7	34.7	32.7	33.7	–			50.7	50.7	50.7	6.0	6.0	6.0
Studies from other regions																			
Fu et al. 2011	American (n = 21)			–			19.1*, †			66.6*			–			14.3*, †			–
Jaffar & Hamadah, 2003	Caucasian (Iraqi) (n = 100)			–			12.0*			19.0*			–			55.0%			14.0%
Malamed & Trieger, 1983	Mixed (n = 316)			–			39.9*			–			–			60.1*			–

GPF, greater palatine foramen; M2, second maxillary molar; M3, third maxillary molar; F, female; M, male; (N), north; (S), south; (E), east; (W), west – referring to the geographical region from which the study samples were collected.

*The authors report total values only.

†The authors describe this location as palatal instead of opposite.

‡The authors report it is 'interproximal to the M1 and M2'.

§This percentage is the sum of what the authors measure to be located between 'the posterior half of the M2 and the anterior half of the M3'.

¶The authors report that the GPF is located 'medial to the M3', however according to the definition given in the manuscript this was reclassified to 'opposite to the M3'.

'R%' and 'L%' – the ratio of the number of GPF in a particular relation to the molar teeth on the right or left sides to all GPF on that side.

'total' – ratio of the total number of GPF on both sides in a particular relation to the molar teeth to the total number of GPF in the examined group.

This table presents the data from 23 relevant studies. The study population from the work of Ajmani [17] has been divided in two, as the study analyses two different populations (African and Indian). Hence the 24 positions in the table.

Table 3 Comparison of studies on the subject of GPF – part I.

Study	Population (number of samples – skulls/ CT scans)	Type of investigation and sample characteristics	GPF dimensions (SD)(mm)		GPF–MMS (SD)(mm)		GPF–PBHP (SD)(mm)		GPF–IF (SD)(mm)		MMS–IF–GPF angle (SD)(°)		Mucosa thickness over GPF (SD)(mm)[¶]	GPF–AR (SD)(mm)		GPF–PH tip (SD)(mm)	
			AP	LM	R	L	R	L	R	L	R	L		R	L	R	L
European studies (total sample $n = 1749$)																	
Tomaszewska et al. 2014 (this study)	Polish ($n = 1350$)	Sinus CT scans ($n = 1200$) Dry human skulls; sexed ($n = 150$) mean age 44.9 ± 17.1 years; Total: 655M, 695F	5.1 (0.5)	3.0 (0.8)	16.1 (1.5) 15.9 (1.5)*	15.6 (1.5)	4.9 (1.0) 4.8 (1.0)*	4.8 (1.0)	34.0 (3.0) 34.2 (3.0)*	34.3 (3.1)	26.0 (2.9) 26.2 (2.9)*	26.3 (3.0)	–	3.0 (1.3) 3.0 (1.2)	2.9 (1.3)	11.9 (1.0) 11.9 (1.1)	12.0 (1.1)
Nimigean et al. 2013	Romanian ($n = 100$)	Dry human skulls; age range 25–40 years; sexed	4.9 (0.9)	3.0 (0.9)	14.5 (0.7)		4.4 (1.1)		–		–		6.0	–		12.0 (1.8)*	
Piagkou et al. 2012	Greek ($n = 71$)	Dry human skulls; adult; unsexed	5.3 (0.9)	2.7 (0.5)	15.3 (1.3)		4.6 (1.0)	4.7 (1.1)	–		–		–	3.1 (1.7)	2.9 (1.6)	–	
African studies (total sample $n = 440$)																	
Osunwoke et al. 2011	Nigerian ($n = 150$)	Dry human skulls; adult; sexed (100%M)	–	15.0 (2.1)	15.0 (2.1)	14.3 (1.5)	5.0 (1.2)	5.1 (5.1)	41.1 (5.0)		–		–	–		–	
Ajmani, 1994	Nigerian ($n = 65$)	Dry human skulls; adult, unsexed	–		15.4 (0.2)	15.4 (0.2)	3.5 (0.2)	3.5 (0.2)	–		–		–	–		–	
Hassanali & Mwaniki, 1984	Kenyan ($n = 125$)	Dry human skulls; adult; sexed (60M, 22F, 43U)	–		–		–		–		–		–	–		–	
Langenegger et al. 1983	South African ($n = 100$)	Dry human skulls; mean age 42.7 years; sexed (50M, 50F)	–	2.5 (0.5)	15.1 (2.6)	14.9 (1.8)	–		–		–		–	–		12.3 (1.8)	12.6 (1.9)
Asian studies (total sample $n = 351$)																	
Hwang et al. 2011	Korean ($n = 50$)	Head HRCT scans; mean age 51.0 years; sexed (22M, 28F)	4.5 (0.7)	2.2 (0.4)	16.2 (1.3) *		–		–		–		10.7 (1.8)	–		–	
Klosek & Rungruang, 2009	Thai ($n = 41$)	Human cadavers; mean age 71.2	F: 5.1 (1.0)	F: 2.8 (1.0)	14.7 (3.3)		–		34.0 (7.3)		–		–	–		–	

Table 3. (continued)

Study	Population (number of samples – skulls/ CT scans)	Type of investigation and sample characteristics	GPF dimensions (SD)(mm)		GPF–MMS (SD)(mm)		GPF–PBHP (SD)(mm)		GPF–IF (SD)(mm)		MMS–IF–GPF angle (SD)(°)		Mucosa thickness over GPF (SD)(mm)[¶]	GPF–AR (SD)(mm)		GPF–PH tip (SD)(mm)	
			AP	LM	R	L	R	L	R	L	R	L		R	L	R	L
		years; sexed (24M, 17F)	M: 4.9 (8.3) 3.25 (0.5) [†]	M: 2.6 (8.3)													
Methathrathip et al. 2005	Thai ($n = 160$)	Dry human skulls ($n = 105$) – mean age 48.1 years; sexed (68M, 37F); Human cadavers ($n = 55$)	4.9 (0.9)	2.7 (0.5)	16.2 (1.3)		2.1 (1.3)		–		–		6.7 (2.3)	–		–	
Wang et al. 1988	Chinese ($n = 100$)	Dry human skulls; adult; sexed	–		16.0 (0.2) 16.0 (0.1)	16.0 (0.1)	3.9 (0.1) 4.1 (0.1)	4.3 (0.1)	–		–		–	–		–	
Brazilian studies (total sample $n = 408$)																	
Ikuta et al. 2013	Brazilian ($n = 50$)	CBCT scans; mean age 35.8 years; sexed (27M, 23F)	3.1[†] (0.5)		15.2 (1.45)		–		–		–		–	7.9 (2.0)		–	
Lopes et al. 2011	Brazilian ($n = 94$)	Dry human skulls; adult; sexed (65M, 29F)	–		15.6 (1.3)	15.4 (1.4)	3.4 (1.2)	3.5 (1.1)	–		–		–	–		–	
Chrcanovic & Custódio, 2010	Brazilian ($n = 80$)	Dry human skulls; age unknown; unsexed	–		14.7 (1.6)	14.4 (1.4)	3.4 (1.1)*		36.2 (3.2)	36.5 (3.3)	22.1 (2.7)	23.3 (2.5)	–	–		–	
Teixeira et al. 2010	Brazilian ($n = 141$)	Dry human skulls; mean age 31.6 ± 13.1 years; sexed (82M, 59F)	–		15.7 (1.6)	16.2 (1.6)	–		39.3 (3.4)	39.1 (3.8)	–		–	–		–	
Urbano et al. 2010	Brazilian ($n = 43$)	Dry human skulls; adult; unsexed	–		16.6	16.4	4.5	4.6	–		–		–	–		–	

Table 3. (continued)

Study	Population (number of samples – skulls/ CT scans)	Type of investigation and sample characteristics	GPF dimensions (SD)(mm)		GPF–MMS (SD)(mm)		GPF–PBHP (SD)(mm)		GPF–IF (SD)(mm)		MMS–IF–GPF angle (SD)(°)		Mucosa thickness over GPF (SD)(mm)[¶]	GPF–AR (SD)(mm)		GPF–PH tip (SD)(mm)	
			AP	LM	R	L	R	L	R	L	R	L		R	L	R	L
Indian studies (total sample $n = 937$)																	
Dave et al. 2013	Indian (W) ($n = 100$)	Dry human skulls; adult; sexed (60M, 39F, 1U)	–		F: 16.2 (1.6) M: 16.7 (1.1)	F: 16.4 (1.1) M: 16.6 (1.1)	F: 6.7 (1.2) M: 6.9 (1.3)	F: 7.0 (1.3) M: 6.9 (1.2)	–		–		–	–		–	
Sharma & Garud, 2013	Indian (W) ($n = 100$)	Dry human skulls; adult; unsexed	4.7 (1.1)	3.25 (0.5) [†]	14.7 (1.4)	14.7 (1.4)	3.4 (1.5)	3.4 (1.5)	35.4 (2.8)	35.7 (2.6)	–		–	–		12.1 (2.5)	11.5 (1.9)
Jotania et al. 2013	Indian (W) ($n = 60$)	Dry human skulls; adult; unsexed	–		14.8 (1.2)	14.8 (1.5)	–		–		–		–	–		–	
D'Souza et al. 2012	Indian (SW) ($n = 40$)	Dry human skulls; adult; unsexed	–		14.6 (1.5)	14.4 (1.4)	–		–		–		–	–		–	
Kumar et al. 2011	Indian (N) ($n = 100$)	Dry human skulls; adult; unsexed	–		14.3 (1.4) 14.3 (1.3) *	14.4 (1.3)	3.6 (0.9) 3.6 (0.9) *	3.6 (0.9)	36.6 (2.2) 36.2 (3.21) *	35.7 (3.9)	–		–	–		–	
Saralaya & Nayak, 2007	Indian (SW) ($n = 132$)	Dry human skulls; adult; unsexed	–		14.7 (0.2) 14.7 (0.3) *	14.7 (0.2)	4.2 (0.1) 4.2 (0.2) *	4.2 (0.1)	37.2 (0.3) 37.3 (0.7) *	37.4 (0.3)	21.1 (4.2) 21.1 (2.0) *	21.1 (4.2)	–	–		–	
Sujatha et al. 2005	Indian (S) ($n = 71$)	Dry human skulls; adult; unsexed	–		–		–		–		–		–	–		–	
Ajmani, 1994	Indian (N) ($n = 34$)	Dry human skulls; adult, unsexed	–		14.7 (1.0)	14.6 (1.1)	3.7 (1.2)	3.7 (1.4)	–		–		–	–		–	
Westmoreland & Blanton, 1982	Indian (E) ($n = 300$)	Dry human skulls; adult; unsexed	–		14.8 (0.1)	15.0 (0.1)	1.9 (0.04)	1.9 (0.04)	–		–		–	–		–	
Studies from other regions																	
Fu et al. 2011	American ($n = 11$)	Fresh cadaver heads; mean age 75.7 years; 100% M	–		–		–		–		–		–	–		–	
		Dry human skulls; adult; unsexed	4.6 (1.0)	2.8 (0.6)	15.7 (1.4) *		4.9[r] (0.1) *[,‡]		–		–		–	–		–	

Table 3. (continued)

Study	Population (number of samples – skulls/ CT scans)	Type of investigation and sample characteristics	GPF dimensions (SD)(mm)		GPF–MMS (SD)(mm)		GPF–PBHP (SD)(mm)		GPF–IF (SD)(mm)		MMS–IF–GPF angle (SD)(°)		Mucosa thickness over GPF (SD)(mm)[¶]	GPF–AR (SD)(mm)		GPF–PH tip (SD)(mm)	
			AP	LM	R	L	R	L	R	L	R	L		R	L	R	L
Jaffar & Hamadah, 2003	Caucasian (Iraqi) ($n = 50$)																
Malamed & Trieger, 1983		Mixed (61.8% European, 27.9% American, 10.3% African) ($n = 204$)	Dry			human skulls; adult; unsexed	–		–		7.0*,[§]		–		–		–
–		12.2*,[§]															

AP, anterior–posterior GPF dimension; AR, alveolar ridge; CBCT, cone-beam computed tomography; F, female; GPF, greater palatine foramen; HRCT, high-resolution computed tomography; IF, incisive foramen; LM, lateral–medial GPF dimension; M, male; MMS, midline maxillary suture; *n*, number; NA, not available; PBHP, posterior border of the hard palate; PH, pterygoid hamulus; SD, standard deviation; U, unknown. (E), east; (N), north; (S), south; (W), west – referring to the geographical region from which the study samples were collected.
This table presents the data from 27 studies containing relevant measurements. The study population from the work of Ajmani (17) has been divided in two, as the study analyses two different populations (African and Indian). Hence the 28 positions in the table.
*Mean value for both sides.
[†]GPF diameter.
[‡]Distance between GPF centre and the most lateral point of the PBHP (in all other studies distance between GPF and the nearest medial aspect of the PBHP).
[§]Authors only measure with an accuracy of 0.5 mm. Range for GPF–PBHP distance 3–12 mm. Range for GPF–PH tip 5.0–20.5 mm.
[¶]Measured only on CT scans.

Table 4 Comparison of studies on the subject of GPF – part II.

Study	Population (number of samples)	GPF opening direction (%)				Palatal vault shape	Mean palatal vault height (SD) (mm)	Mean palatal breadth (SD) (mm)	Mean palate length (SD) (mm)	PI (%)	PHI (%)	GPF posterior palatine crest (%)		Mean LPF number (SD) (range)	
		I-A-M	I-A-L	Anterior	Vertical							R	L	R	L
European studies (total sample $n = 1521$)															
Tomaszewska et al. 2014 (this study)	Polish ($n = 1350$)	82.6	3.8	7.4	5.2	U-shaped 100% Flat: 22.0% Arched: 58.7% High-arched: 19.3%	13.1 (2.7)	46.9 (3.3)	47.0 (4.5)	99.8 (5.4)	30.1 (3.1)	32.4*	30.7*	1.6* (0–5)*	1.5*
Nimigean et al. 2013	Romanian ($n = 100$)	82.0	–	13.0	5.0	–	–	46.9	–	–	–	–		–	
Piagkou et al. 2012	Greek ($n = 71$)	–				–	–	–	–	–	–	57.8	56.3	1.8 (1–5)	1.6
African studies (total sample $n = 440$)															
Osunwoke et al. 2011	Nigerian ($n = 150$)	–				–	–	–	–	–	–	–		1.3 (0.5)	1.2 (0.4)
Ajmani, 1994	Nigerian ($n = 65$)	58.7	38.7	–	–	U-shaped: 100%	30–80 mm	–	–	–	–	24.6†		–	
Hassanali & Mwaniki, 1984	Kenyan ($n = 125$)	74.0	–	–	26	–	12.2 (1.6)	40.2 (3.6)	49.2 (3.6)	82.0 (7.8)	30.3 (6.3)	43.7†		1.6 (0–5)	1.7
Langenegger et al. 1983	South African ($n = 100$)	–				–	–	–	–	–	–	90.0	91.0	–	
Asian studies (total sample $n = 301$)															
Klosek & Rungruang, 2009	Thai ($n = 41$)	–				–	14.8 (3.6)	31.1 (5.2)	51.4 (5.8)	61.0 (13.0)	–	–		–	
Methathrathip et al. 2005	Thai ($n = 160$)	–	–	–	97.6	–	–	–	–	–	–	–		–	
Wang et al. 1988	Chinese (Taiwan) ($n = 100$)	–	–	90.0	10.0	–	–	–	–	–	–	–		–	
Brazilian studies (total sample $n = 80$)															
Chrcanovic & Custódio, 2010	Brazilian ($n = 80$)	18.8	0.0	69.4	11.9	–	–	–	52.4 (4.6)	–	–	–		–	
Indian studies (total sample $n = 866$)															
Dave et al. 2013	Indian (W) ($n = 100$)	–	–	4.0	96.0	–	–	–	–	–	–	–		–	
Jotania et al. 2013	Indian (W) ($n = 60$)	–				–	–	37.8	49.7	76.1	–	–		1.7 (0–4)	1.7
Sharma & Garud, 2013	Indian (W) ($n = 100$)	49.5	3.5	2.0	45.0	–	–	–	–	–	–	32.3 27.8†	23.2	1.4 (0–5)	1.4

Table 4. (continued)

Study	Population (number of samples)	GPF opening direction (%)				Palatal vault shape	Mean palatal vault height (SD) (mm)	Mean palatal breadth (SD) (mm)	Mean palate length (SD) (mm)	PI (%)	PHI (%)	GPF posterior palatine crest (%)		Mean LPF number (SD) (range)	
		I-A-M	I-A-L	Anterior	Vertical							R	L	R	L
D'Souza et al. 2012	Indian (SW) (n =40)	–				–	–	–	–	–	–	–		Single LPF: 62.5% 2 LPF: 30% 3 LPF: 7.5%	
Kumar et al. 2011	Indian (N) (n = 100)	19.0	73.0	1.0	7.0	Flat: 20% Arched: 69% High-arched: 11%	–	–	–	–	–	1.0†		1.2 (0.5) (0–3)	1.3 (0.5)
Saralaya & Nayak, 2007	Indian (SW) (n = 132)	46.2	12.5	41.3	–	Flat: 37.1% Arched: 46.2% High-arched: 16.7%	–	–	–	–	–	–		(1–4)	
Ajmani, 1994	Indian (N) (n = 34)	91.4	–	–	–	U-shaped: 100%	30–80 mm	–	–	–	–	25.3†		–	
Westmoreland & Blanton, 1982	Indian (E) (n = 300)	–	–	18.0	82.0	U-shaped: 100%	40–80 mm	–	–	–	–	16.0†		–	
Studies from other regions															
Fu et al. 2011	American (n = 11)	–				–	14.1 (2.5)	–	–	–	–	–		–	
Jaffar & Hamadah, 2003	Caucasian (Iraqi) (n = 50)	60.0	–	36.0	4.0	–	–	39.3 (3.4)	50.8 (3.6)	77.6 (6.0)	–	67.0%†		Single LPF: 41% multiple LPF: 55% absent LPF: 4%	
Malamed & Trieger, 1983	Mixed (n = 204)	–	–	38.7	61.3	–	–	–	–	–	–	–		–	

F, females; GPF, greater palatine foramen; LPF, lesser palatine foramen/foramina; M, males; SD, standard deviation.GPF opening direction: I-A-M: inferiorly antero-medially; I-A-L: inferiorly antero-laterally.
PI (palatine index): palatine breadth to palatine length ratio (%); PHI (palatine height index): palatine height to palatine breadth ratio (%).
Palatine breadth: measured at the level of maxillary second molars. Palatine length: distance between the orale and staphylion points.
This table presents the data from 21 studies containing relevant measurements. The study population from the work of Ajmani (17) has been divided in two, as the study analyses two different populations (African and Indian). Hence the 22 positions in the table.
*Measured only in 150 dry, adult skulls.
†Mean value for both sides.

included in the meta-analysis, as four studies did not relate the GPF to the maxillary molars.

Considering the most common GPF position – opposite the M3 – the *Q*-test showed high heterogeneity ($Q = 744.7$; $P < 0.0001$), as confirmed by the I^2-test (96.9%; 95% CI = 96.2–97.5%) for the 23 studies included in the meta-analysis (Fig. 3). However, both Egger's ($P = 0.16$) and Begg's tests ($P = 0.21$) did not indicate the presence of study bias. Thus, the pooled prevalence of the GPF being positioned opposite the M3 was calculated to be 63.9% (95% CI = 56.6–70.9%; Fig. 4).

To explore the source of the heterogeneity, the studies were subdivided into groups based on geographical location. For European studies, the *Q*-test showed almost no heterogeneity ($Q = 0.36$; $P = 0.84$), confirmed by the I^2-test (0.0%). For the rest of the geographical regions, the heterogeneity was still medium to high: for African studies $Q = 236.7$ ($P < 0.0001$), $I^2 = 98.72\%$ (95% CI = 98.2–99.1%); for Asian studies $Q = 45.7$ ($P < 0.0001$), $I^2 = 95.6\%$ (95% CI = 91.6–97.7%); and for Indian studies $Q = 208.5$ ($P < 0.0001$), $I^2 = 96.2\%$ (95% CI = 94.4–97.4%). Figure 5 depicts a forest plot for studies pooled in groups according to the geographical region they originated from. However, due to manual choosing of the studies, selectivity publication bias appeared: Egger's test ($P = 0.005$) and Begg's test ($P = 0.09$).

Discussion

As mentioned earlier, classic anatomical or surgical textbooks localize the GPF in a very general manner, leading to inconsistencies in physician training. The majority of studies regarding GPF position have been conducted on dry adult skull, thus delivering limited information on the gender and age of the samples (Table 3). Though our study has shown that measurements conducted on dry skulls are equal to those performed on CT scans, the latter method has the added value of knowing the participants exact age, gender, ethnicity and very often other important medical parameters. It also allows to gather a substantially larger patient sample for statistical analysis.

Though many studies (Table 3) have been conducted on the subject of GPF location, new clinical reports are constantly published stating the difficulties with locating this anatomical reference point (Piagkou et al. 2012; Ikuta et al. 2013). The anatomy of the GPF is bound to gain even more attention, as through the GPF it is possible to stimulate the pterygopalatine ganglion (Piagkou et al. 2012). This can be used in stroke patients to reduce the stroke's effect, but also to intervene in patients with cluster and migraine headaches, as well as cerebral vasospasm conditions (Oluigbo et al. 2011). From the clinical point of view, it should be stressed that in-depth knowledge of GPF anatomy is mandatory, as this is the most important site in the palate, having the greatest and most precise representation in the somatosensory cortex (Bessho et al. 2007).

According to the literature search, this study is by far the largest to date: both in terms of the number of samples and measurements. It has shown that the GPF is most often located opposite the M3 – on average in two-thirds to three-quarters of all patients, both in Europe and worldwide. The prepared systematic review and meta-analysis will be of great value to clinicians, allowing to adequately prepare oneself before performing procedures using the GPC approach or in the vicinity of the GPF. Even if one of the molar teeth is missing, the other reference points will supply enough data to easily localize the GPF. Additionally, this study has brought to light the fact that the position of the GPF, as well as its distance from certain anatomical reference points, might be used to distinguish between male and female skulls during forensic examination.

Location of the GPF in relation to the maxillary molars

The first attempt to reference the GPF to other anatomical points was undertaken by Matsuda (1927) on a mixed ethnical sample of 380 skulls. Slavkin et al. (1966) noted that the GPF moves posteriorly with the eruption of new teeth in children. This was the reason why we chose not to include specimens/scans from patients younger than 21

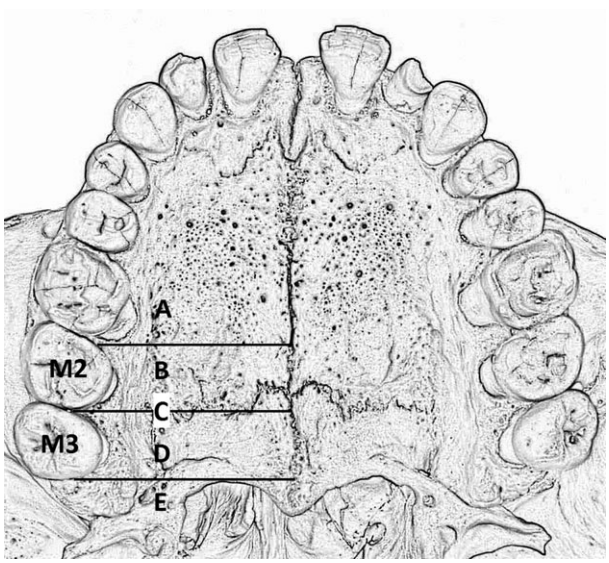

Fig. 6 Classification of the GPF position in relation to the maxillary molars. (A) Mesial to the second maxillary molar (M2; mesial/anterior to the mesial surface of the M2); (B) opposite (medial) the M2 (from the mesial surface of the M2 to the distal surface of the M2); (C) between (interproximal) the M2 and the third maxillary molar (M3; at the level of the contact surface between the M2 and the M3); (D) opposite (medial) the M3 (from the mesial surface of the M3 to the distal surface of the M3); (E) distal to the M3 (distal/posterior to the distal surface of the M3).

years. Although numerous studies have been conducted, there is still no agreement as to whether the position of the GPF is prone to ethnical variability, with Wang et al. (1988) and Chrcanovic & Custudio (2010) supporting this claim with their studies, and Jaffar & Hamadah (2003) refuting this theory. Though the heterogeneity of the studies included in our meta-analysis might suggest that the diversity may be due to genetic factors, we should look to the subgroup analysis for the more probable answer. European studies show no heterogeneity at all in terms of the position of the GPF, even though they originate from different regions, whereas Indian studies (Saralaya & Nayak, 2007; D'Souza et al. 2012; Dave et al. 2013; Jotania et al. 2013; Sharma & Garud, 2013) conducted on the same population from one western state demonstrate significant heterogeneity. After analysing all of the studies, and the measurements they performed, we think that the causes of GPF position diversity are differences in the quality of measurements performed, as well as the way the GPF was related to the maxillary molars. That is why we would like to introduce a unified classification that would help to position the GPF in relation to the maxillary molars. The position of the GPF in relation to the maxillary molars should be assessed as described in the Materials and methods, and the possible GPF position would be one of the five listed below (Fig. 6).

1 (A) Mesial to the M2 (mesial/anterior to the mesial surface of the M2).
2 (B) Opposite (medial) the M2 (from the mesial surface of the M2 to the distal surface of the M2).
3 (C) Between (interproximal) the M2 and the M3 (at the level of the contact surface between the M2 and the M3).
4 (D) Opposite (medial) the M3 (from the mesial surface of the M3 to the distal surface of the M3).
5 (E) Distal to the M3 (distal/posterior to the distal surface of the M3).

An additional aspect to consider when referencing the GPF to the maxillary molars is the shape of the GPF. In most populations the GPF is elongated (Langenegger et al. 1983; Ajmani, 1994; Klosek & Rungruang, 2009) rather than oval in shape. It is important to measure the relation of the GPF centre to the maxillary molars, rather than one of its borders. To assist researchers in designing future studies, a detailed description of how to determine the centre of the GPF has been given in the Materials and methods.

GPF–MMS, GPF–PBHP, GPF–PH and MMS–IF–GPF angle measurements

The GPF–MMS and GPF–PBHP measurement values found in this study demonstrate rather significant inter-population variability (Table 3). Slavkin et al. (1966) stated that GPF location variability may occur due to sutural growth between the maxilla and the palatine bone. We also have to bear in mind that the antero-posterior dimension of the palate increases with the eruption of the posterior teeth.

Hawkins & Isen (1998) have described the location of the GPF to be along a straight line from the tip of the PH to the ipsilateral cingulum of the lateral incisor (Fig. 1). The PH is palpable on the postero-lateral side of the soft palate, about 2 mm posteriorly from the pterygomaxillary suture (Nimigean et al. 2013). Thus, we consider the tip of the PH an accurate reference point, located consistently throughout different studies about 12 mm in a straight line from the GPF (Table 3).

The MMS–IF–GPF angle values found in our study differ from those found by Chrcanovic & Custudio (2010) (right = 22.12 °; left = 23.30 °) and Saralaya & Nayak (2007) (right = 21.1 °; left = 21.2 °). Though statistically significant differences were found between the right and left angles, these discrepancies still remain clinically insignificant. Taking into account the ease with which the MMS can be located, the knowledge of the mean value of the MMS–IF–GPF angle will help physicians determine the angle at which the needle should be introduced into the GPF.

Locating the GPF in edentulous patients

When palpating for the GPF in edentulous patients, we would suggest triangulating the position of the GPF using the AR, MMS and the PNS, as they are constant and easily identifiable. The tip of the PH can also be added as an extra reference point. Though the posterior margin of the hard palate is clinically visible due to a narrow mucous membranous band of lighter colour (Nimigean et al. 2013) corresponding to it, we do not recommend using it as a reference point, as it is not clinically practical. The differences in the GPF–PBHP distance can be explained by growth at the level of the transverse palatine suture, and by the fact that palate length increases anteriorly from this suture after lateral teeth eruption. At the same time, growth is significantly reduced posteriorly from this line (Nimigean et al. 2013). Another explanation lies in the fact that some authors refer the GPF to the lateral-most aspect of the PBHP (Jaffar & Hamadah, 2003), while others to the greatest concavity of the PBHP (Westmoreland & Blanton, 1982; Ajmani, 1994).

When clinically utilizing all of the mentioned reference points and measurements given, the needle traverses the shortest possible route before administering the anaesthetic. The physician also avoids the risk of creating a haematoma resulting from pterygoid plexus vein puncture, as well as the possibility of anaesthetic deposition into the fat pad (Yamamoto et al. 2004).

Opening direction of the GPF

The inter-study comparison of the opening direction of the GPF (Table 4) proved to be difficult, as authors used different estimation methods. That is why we cannot agree with the statement of Wang et al. (1988) that the discrepancies are due to racial variations. The only sure way to determine the opening direction of the GPF is to base on horizontal and sagittal CT scans. Assessments utilizing dry skulls and needles only provide a very rough estimate of the GPF opening direction. Further CT-based studies are needed to accurately assess the opening direction of the GPF in different populations. In our study, vertical GPF openings were rather rare; however, their existence may explain the occasional clinical difficulty encountered while attempting to insert the needle point into the GPF and the pterygopalatine canal. Additionally, according to Slavkin et al. (1966), the frequency of anatomical obstruction of the needle in the GPC increases with age.

Posterior palatine crest of the GPF and the LPF

The presence of the posterior palatine crest is highly variable between studies (Table 4). This is where palatal tendons and muscles attach (Hassanali & Mwaniki, 1984). The posterior palatine crest, if present, may act as a natural barrier preventing the needle from venturing into the nasopharynx (Malamed & Trieger, 1983). Jaffar & Hamadah (2003) consider the presence of the posterior palatine crest important in prosthetic dentistry, but taking into account the thickness of the mucosa covering the GPF and the resulting minimal risk of developing pressure lesions in patients with removable dental prostheses, we think this finding is of no clinical significance.

We did not find any literature data suggesting that the number of LPFs may have clinical meaning. However, the absence of LPF, as it was found in this and several other studies (Table 4), may cause the lesser palatine nerve to exit through the GPF, and thus be prone to anaesthesia when blocking the greater palatine nerve. On the other hand, a high number of LPFs may lead to the formation of a single large LPF, as Jaffar & Hamadah (2003) have found. Such an anatomical variation may lead to mistaking the LPF for the GPF, and thus anaesthetizing the lesser palatine nerve, leading to a gagging sensation in the soft palate (Hassanali & Mwaniki, 1984).

Gender- and side-related differences

Male skulls are generally larger and more massive than female ones (Teixeira et al. 2010). Analysis of the obtained results has shown that most of the GPF-related measurements significantly differ between sexes (Table 1). This shows that the position of the GPF in relation to other anatomical landmarks could be used in forensic examination to identify a person's sex. Our study has shown that the GPF–MMS and the GPF–IF distances differ between sides. This stands in agreement with the study of Teixeira et al. (2010), but disagrees with some of the other studies included in the systematic review (Jaffar & Hamadah, 2003; Methathrathip et al. 2005; Saralaya & Nayak, 2007). These differences might be the result of palatal development, which is dependent on the function of several ossification centres (Slavkin et al. 1966).

Strong sides, limitations and novelty of the current study

The strong sides of the present project included the largest study sample size and number of individual measurements performed of all the studies published up-to-date on the subject of GPF position. The CT scan vs. traditional dry skull measurements comparison, as well as random measurement verification, were further factors guaranteeing high precision of the results. The use of CT scans allowed to gather data on the patients' sex and age. Finally, the systematic review was performed according to PRISMA guidelines, and the subsequent meta-analysis of observational studies was the very first regarding GPF position, and created a unified, clinically useful review of all pertinent studies.

Several limitations of the present study should also be mentioned. Most of the included studies had small study groups. Heterogeneity among studies may be another limitation of our meta-analysis; however, we applied a random-effects model that takes possible heterogeneity into consideration (Xia et al. 2014). Exclusion of conference abstracts and non-English language studies may have led to publication bias; however, the performed statistical tests showed no bias was present in the performed meta-analysis. Despite these limitations, meta-analysis is a cost-effective and reasonable approach to evaluating sporadic, inconsistent and small sample size studies (Xu et al. 2014).

The novelty of this study stems from its design – it is the first systematic review and meta-analysis on the subject of GPF position, with added original data. Utilizing such an approach, the authors were able to present, for the first time, the pooled prevalence of GPF position in relation to the maxillary molars – both in the general world population, as well as divided by geographical regions. Following, the authors developed a clear, concise, easy to use and most importantly unambiguous classification system of positioning the GPF in relation to the maxillary molars. This study is also the first to present a straightforward methodology of determining the centre of the GPF, thus allowing to conduct reliable and repetitive measurements in future studies regarding GPF anatomy. The pooled data presented in this manuscript will allow clinicians to adequately prepare before performing

procedures using the GPC approach or in the vicinity of the GPF, regardless of the geographical region they are working in. Finally, this study presents evidence that GPF position may not be so prone to anatomical variability. The large discrepancies between certain studies originate rather from differences in measurement methodology. By implementing the above-mentioned classification and methodology, this study aims to prevent such discrepancies from occurring in future studies regarding GPF anatomy.

Conclusions

Concluding, a clear understanding of the location and anatomy of the GPF is needed in order to properly administer anaesthetic through this foramen during maxillofacial procedures. Using a systematic review and meta-analysis, we demonstrated that the GPF is most often located opposite the M3 in the majority of the world's populations. In Poles, the GPF is located approximately 11 mm in a straight line from the M3. The maxillary molars are the best landmarks for locating the GPF. In edentulous patients the most useful points for approximating the position of the GPF are the AR, MMS and the PNS. Taking into account the estimated location of the GPF, clinicians should remember that when harvesting a palatal mucosa graft, they should avoid crossing the distal surface of the M2. Additionally, this study introduces an easy and repeatable classification to reference the GPF to the maxillary molars. Further CT-based studies are needed to estimate the opening direction of the GPF in different populations.

Conflict of interest statement

All authors declare that they have no conflict of interest or financial relationship to disclose.

Acknowledgements

The authors wish to thank Mr Jacenty Urbaniak for his excellent photographs.

Funding

This study has been funded using Jagiellonian University statutory funds. Krzysztof A. Tomaszewski received a scholarship to prepare his PhD thesis from the National Science Center, Poland under award number DEC-2013/08/T/NZ5/00020.

Author contributions

Design and planning of the study: IMT, MN, JAW. Data collection (measuring the samples): IMT, KAT, EKK, IZP, MN. Data interpretation: IMT, KAT (statistics and radiological interpretation); AU (radiological interpretation). Bibliographic search: IMT, JAW. Drafting and revising the manuscript: IMT. Obtaining funding and critical revision of the manuscript: MN, JAW. All authors have read and approved the final version of the manuscript. All co-authors confirm the above-mentioned contributions and consent to the fact that this study is a part of Iwona M. Tomaszewska's PhD thesis. The co-authors confirm that Iwona M. Tomaszewska has contributed significantly (70% in total) to every part of this study, as stated above.

References

Ajmani ML (1994) Anatomical variation in position of the greater palatine foramen in the adult human skull. *J Anat* **184**, 635–637.

Aterkar S, Rawal PM, Kumar P (1995) Position of greater palatine foramen in adults. *J Anat Soc India* **44**, 126–133.

Bell G (2011) Oro-antral fistulae and fractured tuberosities. *Br Dent J* **211**, 119–123.

Bessho H, Shibukawa Y, Shintani M, et al. (2007) Localization of palatal area in human somatosensory cortex. *J Dent Res* **86**, 265–270.

Chrcanovic BR, Custódio AL (2010) Anatomical variation in the position of the greater palatine foramen. *J Oral Sci* **52**, 109–113.

Das S, Kim D, Cannon TY, et al. (2006) High-resolution computed tomography analysis of the greater palatine canal. *Am J Rhinol* **20**, 603–608.

Dave MR, Yagain VK, Anadkat S (2013) A study of the anatomical variations in the position of the greater palatine foramen in adult human skulls and its clinical significance. *Int J Morphol* **31**, 578–583.

Douglas R, Wormald PJ (2006) Pterygopalatine fossa infiltration through the greater palatine foramen: where to bend the needle. *Laryngoscope* **116**, 1255–1257.

D'Souza AS, Mamatha H, Nayak J (2012) Morphometric analysis of hard palate in south Indian skulls. *Biomed Res* **23**, 173–175.

Egger M, Davey Smith G, Schneider M, et al. (1997) Bias in meta-analysis detected by a simple, graphical test. *BMJ* **315**, 629–634.

Fu JH, Hasso DG, Yeh CY, et al. (2011) The accuracy of identifying the greater palatine neurovascular bundle: a cadaver study. *J Periodontol* **82**, 1000–1006.

Hassanali J, Mwaniki D (1984) Palatal analysis and osteology of the hard palate of the Kenyan African skulls. *Anat Rec* **209**, 273–280.

Hawkins JM, Isen D (1998) Maxillary nerve block: the pterygopalitine canal approach. *J Calif Dent Assoc* **26**, 658–664.

Howard-Swirzinski K, Edwards PC, Saini TS, et al. (2010) Length and geometric patterns of the greater palatine canal observed in cone beam computed tomography. *Int J Dent*. doi: 10.1155/2010/292753.

Huedo-Medina TB, Sánchez-Meca J, Marín-Martínez F, et al. (2006) Assessing heterogeneity in meta-analysis: Q statistic or I^2 index? *Psychol Meth* **11**, 193–206.

Hwang SH, Seo JH, Joo YH, et al. (2011) An anatomic study using three-dimensional reconstruction for pterygopalatine fossa infiltration via the greater palatine canal. *Clin Anat* **24**, 576–582.

Ikuta CR, Cardoso CL, Ferreira-Júnior O, et al. (2013) Position of the greater palatine foramen: an anatomical study through cone beam computed tomography images. *Surg Radiol Anat* **35**, 837–842.

Jaffar AA, Hamadah HJ (2003) An analysis of the position of the greater palatine foramen. *J Basic Med Sci* **3**, 24–32.

Jotania B, Patel SV, Patel SM, et al. (2013) Morphometric analysis of hard palate. *Int J Res Med* **2**, 72–75.

Klosek SK, Rungruang T (2009) Anatomical study of the greater palatine artery and related structures of the palatal vault: considerations for palate as the subepithelial connective tissue graft donor site. *Surg Radiol Anat* **31**, 245–250.

Kumar A, Sharma A, Singh P (2011) Assessment of the relative location of greater palatine foramen in adult Indian skulls: consideration for maxillary nerve block. *Eur J Anat* **15**, 150–154.

Langenegger JJ, Lownie JF, Cleaton-Jones PE (1983) The relationship of the greater palatine foramen to the molar teeth and pterygoid hamulus in human skulls. *J Dent* **11**, 249–256.

Lee SP, Paik KS, Kim MK (2001) Variations of the prominences of the bony palate and their relationship to complete dentures in Korean skulls. *Clin Anat* **14**, 324–329.

Lopes PTC, Santos AMPV, Pereira GAM, et al. (2011) Morphometric analysis of the greater palatine foramen in dry Southern Brazilian adult skulls. *Int J Morphol* **29**, 420–423.

Malamed SF, Trieger N (1983) Intraoral maxillary nerve block: an anatomical and clinical study. *Anesth Prog* **30**, 44–48.

Matsuda Y (1927) Location of the dental foramina in human skulls from statistical observations. *Int J Orthod Oral Surg Radiogr* **13**, 299–305.

Mercuri LG (1979) Intraoral second division nerve block. *Oral Surg Oral Med Oral Pathol* **47**, 109–113.

Methathrathip D, Apinhasmit W, Chompoopong S, et al. (2005) Anatomy of greater palatine foramen and canal and pterygopalatine fossa in Thais: considerations for maxillary nerve block. *Surg Radiol Anat* **27**, 511–516.

Nimigean V, Nimigean VR, Buţincu L, et al. (2013) Anatomical and clinical considerations regarding the greater palatine foramen. *Rom J Morphol Embryol* **54**, 779–783.

Oluigbo CO, Makonnen G, Narouze S, et al. (2011) Sphenopalatine ganglion interventions: technical aspects and application. *Prog Neurol Surg* **24**, 171–179.

Osunwoke EA, Amah-Tariah FS, Bob-Manuel IF, et al. (2011) A study of the palatine formane in dry human skulls in south-south Nigeria. *Scientia Africana* **10**, 98–101.

Piagkou M, Xanthos T, Anagnostopoulou S, et al. (2012) Anatomical variation and morphology in the position of the palatine foramina in adult human skulls from Greece. *J Craniomaxillofac Surg* **40**, e206–e210.

Rodella LF, Buffoli B, Labanca M, et al. (2012) A review of the mandibular and maxillary nerve supplies and their clinical relevance. *Arch Oral Biol* **57**, 323–334.

Romanes GJ (1981) *Cunningham's Textbook of Anatomy*, 12th edn, p. 116. New York: Oxford University Press.

Saralaya V, Nayak SR (2007) The relative position of the greater palatine foramen in dry Indian skulls. *Singapore Med J* **48**, 1143–1146.

Shane SME (1975) *Principles of Sedation, Local and General Anesthesia in Dentistry*, 1st edn, p. 173. Illinois: The Charles C Thomas Company.

Sharma NA, Garud RS (2013) Greater palatine foramen–key to successful hemimaxillary anaesthesia: a morphometric study and report of a rare aberration. *Singapore Med J* **54**, 152–159.

Slavkin HC, Canter MR, Canter SR (1966) An anatomic study of the pterygomaxillary region in the craniums of infants and children. *Oral Surg* **21**, 225–235.

Sujatha N, Manjunath KY, Balasubramanyam V (2005) Variations of the location of the greater palatine foramina in dry human skulls. *Indian J Dent Res* **16**, 99–102.

Teixeira CS, Souza VR, Maques CP, et al. (2010) Topography of the greater palatine foramen in macerated skulls. *J Morphol Sci* **27**, 88–92.

Urbano ES, Melo KA, Costa ST (2010) Morphologic study of the greater palatine canal. *J Morphol Sci* **27**, 102–104.

Wang TM, Kuo KJ, Shih C, et al. (1988) Assessment of the relative locations of the greater palatine foramen in adult Chinese skulls. *Acta Anat (Basel)* **132**, 182–186.

Westmoreland EE, Blanton PL (1982) An analysis of the variations in position of the greater palatine foramen in the adult human skull. *Anat Rec* **204**, 383–388.

Wong JD, Sved AM (1991) Maxillary nerve block anaesthesia via the greater palatine canal: a modified technique and case reports. *Aust Dent J* **36**, 15–21.

Xia H, Wang X-J, Zhous Q, et al. (2014) Efficacy and safety of talc pleurodesis for malignant pleural effusion: a meta-analysis. *PLoS ONE* **9**, e87060.

Xu H, Guan J, Yi H, et al. (2014) A systematic review and meta-analysis of the association between serotonergic gene polymorphisms and obstructive sleep apnea syndrome. *PLoS ONE* **9**, e86460.

Yamamoto M, Curtin HD, Suwansa-ard P, et al. (2004) Identification of juxtaforaminal fat pads of the second division of the trigeminal pathway on MRI and CT. *Am J Roentgenol* **182**, 385–392.